Application of a full-scale wood gasification biochar as a soil improver to reduce organic pollutant leaching risks

Short title: Full-scale gasification biochar reduces soil pollutant leaching risks

Bao-Son Trinh [a,b,c*], *David Werner* [b], *Brian J. Reid* [c,d]

[a] Institute for Environment and Resources, Vietnam National University of Hochiminh city, HCMC, VN

[b] School of Civil Engineering and Geosciences, Newcastle University, Newcastle upon Tyne, NE1 7RU, UK

[c] School of Environmental Sciences, University of East Anglia, Norwich, NR4 7TJ, UK

[d] Institute of Urban Environment, Chinese Academy of Sciences, Xiamen, P.R. China

[*] Corresponding author: son.trinh@newcastle.ac.uk or trinhbao_son@yahoo.com[1]

[1] Current address: Visiting researcher at Newcastle University

Permanent address: Institute for Environment and Resources, Vietnam National University of Hochiminh city, HCMC, VN

Abstract:

BACKGROUND: The application of biochar to sandy loam soil to reduce leaching of three representative pollutants (a persistent hydrocarbon (phenanthrene; logK_{OW} 4.46), a herbicide (isoproturon; logK_{OW} 2.50), and an antibiotic (sulfamethazine; logK_{OW} 0.28)) were investigated. The wood-derived biochar evaluated in our laboratory study was the solid co-product of a full-scale gasifier feeding a combined heat and power plant. The research aimed to demonstrate multiple environmental benefits with the innovative use of this biochar as a soil improver.

RESULTS: Batch sorption experiments indicated 5% biochar added to soil enhanced the partitioning coefficient (K_d) by factors of 2 for phenanthrene and 20 for both sulfamethazine and isoproturon. Column leaching experiments indicated a reduced porewater flow rate, up to 80% slower in the column amended with 5% biochar, and reduced pollutant leaching risks. Numerical models interlinked batch and column study observations.

CONCLUSION: (i) Biochar enhanced sorption for the hydrophobic pollutant phenanthrene, and also the less hydrophobic pollutants sulfamethazine and isoproturon; (ii) reduced porewater flow rates following biochar amendment gave rise to greater opportunity for pollutant-solid interaction; (iii) mixing with soil resulted in biochar fouling affecting pollutant partition, and (iv) irreversible retention of pollutants by the soil was an important mechanism affecting pollutant transport.

Keywords: char, persistant organic pollutants (POPs), sorption, diffusion, mass transfer, modelling

Abbreviations: Biochar – BC; sulfamethazine – SMZ; isoproturon – IPU; phenanthrene – PHE;

Introduction

Biochar is an organic product formed through the heating of biomass, or other organic wastes, to above 250 ºC, in the absence of (or with limited) oxygen. Biochars are being promoted as beneficial soil improvers, sustainable sorbents and an avenue for greenhouse gas mitigation.[1] As a pyrogenic carbonaceous material, biochar owes its high affinity and capacity for sorbing organic compounds to properties such as high porosity, high specific surface area and/or various functional groups.[2-4] Biochar amendment has been shown to enhance soil sorption affinity and capacity toward organic pollutants which are strongly bound and considered unavailable to further leaching or assimilation by surrounding organisms.[5] Such observations have been shown for organic pollutants that represent a plethora of both hydrophilic[6-8] and hydrophobic compounds.[8-10] Given its advantageous properties, biochar has been studied for a wide-range of environmental management purposes, i.e., for agricultural application to control the leaching of pesticides and pharmaceuticals;[7, 11] for stormwater infiltration systems to retain trace organic pollutants in rain gardens;[8, 12] and for contaminated soil/sediment remediation to minimize pollutant availability and transfer into the food-chain.[3, 13, 14]

In the context of these applications, understanding biochar effects on retention and migration of organic pollutants in biochar amended soil is essential to achieve the desired benefits; for instance, contaminated soil remediation and mitigation of groundwater contamination risk. Several previous studies reported biochar effects on the fate and behavior of organic pollutants in contaminated soils and sediments.[6-10, 15] Others also reported numerical models describing mass transfer processes of several hydrophobic organic contaminants,[16-18] petroleum hydrocarbon vapors,[15, 19] and stormwater trace organic pollutants[8] in biochar/activated carbon amended soils or sediments.

However, few studies use biochars produced as co-products of full-scale renewable energy generation; more commonly these studies use small batches of material produced under well-controlled and optimized laboratory conditions. Optimized conditions may yield high quality biochar with properties which would, however, often not be representative of real-world applications, where the primary design aim is biogas production for bioenergy generation. Furthermore, biochar effects on the retention and leaching of organic pollutants during high infiltration flow events, when groundwater pollution risks are high, has to the best of our knowledge not yet been properly investigated. Addressing these issues is important for two reasons in particular. Firstly there is a need to identify beneficial use opportunities for biochar produced as a co-product under industrial scale renewable energy generation conditions in order to realize multiple environmental benefits, working towards a "zero waste" circular economy. Secondly pollutant leaching under high flow rates, is expected to represent a worst-case scenario for pollutant leaching risks, when mass-transfer limitations will significantly reduce the effectiveness of both soil and biochar to sorb pollutants. These mechanisms, once identified, may have to be incorporated in updated pollutant fate models to accurately predict biochar amendment benefits in soil.

To evaluate the suitability of the solid co-product of renewable energy generation as a cost-effective sustainable sorbent and a beneficial soil improver, batch sorption kinetics and column leaching experiments were undertaken using biochar from a full-scale gasification plant and three representative organic pollutants, namely, phenanthrene (PHE), isoproturon (IPU) and sulfamethazine (SMZ). The chemicals were selected based upon their contrasting physico-chemical properties and their environmental significance. SMZ, a hydrophilic antibiotic pharmaceutical (log K_{OW} 0.28), is one of the most commonly used veterinary drugs and has been

detected with ubiquity in aquatic and terrestrial environments.[20] IPU, a moderately hydrophobic herbicide (log K_{OW} 2.5), has historically been a very high usage herbicide in the EU; it is relatively mobile in the environment and as a consequence has caused frequent breaches of the 0.1 μg l^{-1} European Union limit of pesticides in surface water.[21] PHE, a hydrophobic polycyclic aromatic hydrocarbon (log K_{OW} 4.46), along with 15 other PAHs, is listed by the United States Environmental Protection Agency as priority pollutant.[22] A novel three-domain mass transfer conceptual model was developed to interlink the batch sorption and column leaching studies and gain new insights into the effect of biochar on the transport and fate of organic pollutants in soil.

Materials and Methods

Materials

Soil. A sandy loam soil (21% silt, and 79% sand) was collected from a pasture field at the Norwich Research Park (52°37'N 1°14'E). This site had no history of significant exposure to antibiotics, pesticides or PAHs. The soil was taken from the upper 20 cm of the A-horizon then air-dried (48 h, 20 °C) and sieved (2 mm).

Biochar. Biochar was obtained, using softwood chips as feedstock, from a gasifier that fed a 1.4 MW output Combined Heat and Power Plant (University of East Anglia). The gasification zone operated under negative pressure (2-3 mbar) at around 500 °C. Contrary to the biochars used in previous studies,[8, 15, 19] this biochar represents a real co-product of renewable energy generation from a full-scale gasifier. Thus, application of this biochar would holistically realize multiple environmental benefits, including bioenergy generation, carbon sequestration, and soil improvement, as suggested by Lehmann and Joseph.[1] The biochar was ground by mortar and pestle and then sieved (< 2 mm) for handling and mixing with soil.

Figure 1 presents scanning electron micrograph images of representative soil and biochar grains observed by a SEM Jeol JSM-5900LV. Fundamental physico-chemical properties of these materials are provided in Table 1.

Biochar-soil mixture. Biochar was amended to soil and thoroughly mixed with a spatula in a glass beaker to achieve biochar contents of 0% (BC0 – original soil), 1% (BC1), 5% (BC5) and 100% (BC100 – biochar only) (by weight).

Chemicals. Suppliers and physico-chemical properties of SMZ, IPU, PHE, and their ^{14}C-radiolabeled analogues are presented in Supporting Information and Table S1. ^{12}C- stock solutions of SMZ, IPU and PHE were prepared in acetone with the nominal concentration of 1 g l^{-1}. ^{14}C-radiolabeled stocks were also separately prepared in acetone such that 100 µl would deliver 1 kBq of ^{14}C-SMZ, ^{14}C-IPU or ^{14}C-PHE.

Batch sorption kinetic experiment

The apparent partitioning coefficients ($K_{d,app}$) of SMZ, IPU, and PHE were determined according to the laboratory sorption batch method.[23] For each assessment, BC0, BC1, BC5, and BC100 (3 g, triplicated) were transferred into Teflon centrifuge tubes containing 0.01 M $CaCl_2$ solution with 0.02% sodium azide biocide (30 ml). The stocks were then added to the tubes to achieve a nominal initial concentration of 0.1 mg l^{-1} of ^{12}C-compound and 10 MBq l^{-1} of ^{14}C-compound. Un-spiked tubes (triplicated) were prepared to provide background ^{14}C-counts. The Teflon tubes (covered by foil to reduce photo-degradation) were then placed on their sides and shaken for 0.5, 1, 12, 24, 168, and 720 h in the case of BC0, BC1 and BC5 treatments and for 24, 168, and 720 h in the case of BC100 treatments (100 rpm, IKA Labortechnik KS501). The tubes were then centrifuged (2500 rpm, 20 minutes, Biofuge Stratos Heraeus) and supernatants then

filtered (0.45 µm Satorios). The aqueous filtrate (10 ml) was transferred to a scintillation vial and liquid scintillation cocktail (10 ml UtimaGold XR) was added. The samples were placed in the dark (24 h) before measuring their ^{14}C-radioactivity by liquid scintillation counting (Perkin-Elmer Tri-Carb 2900TR).

Column leaching experiment

A set-up of the column leaching experiment is presented in Figure S1. The glass columns (14 cm length, 3.3 cm ID) were packed with BC0, BC1, and BC5 mixtures (80 g, triplicated). They were saturated by distilled water and left overnight prior to use. The 'feeding' solutions of SMZ, IPU, and PHE in distilled water were individually prepared from the stock solutions to deliver a final nominal concentration of 0.1 mg l^{-1} of the ^{12}C-compounds and 10 MBq l^{-1} of the ^{14}C-compounds. Due to short experimental duration (up to 4 hours), no biocide was added to these feeding solutions. To simulate rapid infiltration as might occur where water ponds on top of soil during heavy rainfall events, and when leaching risks are highest, the 'feeding' solution (100 ml) was loaded onto the top of the columns and then gravitationally drained downward through the columns. Nine further aliquots (each 100 ml) of distilled water were consecutively added to the columns to elute the compounds. Eluted solutions (100 ml) were collected at bottom of the columns and portions (10 ml) of these were transferred into 20 ml scintillation vials and added liquid scintillation cocktails (10 ml UtimaGold XR). These samples were placed in the dark (24 h) before measuring their ^{14}C-radioactivity by a liquid scintillation counter (Perkin-Elmer Tri-Carb 2900TR). The remaining sediment in the PHE column treatments was divided into six equal segments of 1 cm length. These segments were then oxidized by the Packard Model 307 Sample Oxidizer and the absorbed solutions were analysed for ^{14}C-radioactivity by the same liquid scintillation counter (Perkin-Elmer Tri-Carb 2900TR).

Batch and column numerical models

Two numerical models were developed to simulate the fate and transport of the organic pollutants in the batch sorption kinetic and column leaching experiments. These models are based on previously developed concepts accounting for the effects of sorbent amendment (activated carbon or other black carbon materials like char) on the organic pollutant fate in sediments and aquifers,[8, 16, 17, 24, 25] but additionally include irreversible sorption to the soil matrix as a mechanism necessary to explain the experimental observations.

Batch sorption kinetic numerical model. Figure 2A presents a three-domain, namely biochar, soil, and external water, conceptual model which simulates the mass transfer processes of the pollutants in the batch sorption kinetic experiment. It is assumed that the mass transfer processes from external water to soil particles is presented by (1) reversible and (2) irreversible first-order kinetic sorption, and the mass transfer process from external water to biochar particles is presented by (3) sorption-retarded intraparticle diffusion of the pollutant in the pore network of the biochar particles. For the simulation of the pollutant intraparticle diffusion, the biochar particles are divided into concentric spherical shells (Figure 2A), and within each of these subvolumes, a local sorption equilibrium between the biochar solid matrix and pore water is assumed.

The reversible mass transfer rate of the pollutant from external water to soil particles, $r_{s,rev}$ (moles s^{-1}), is described by

$$r_{s,rev} = -V_w k_{s,rev} \left(\frac{C_{s,rev}}{K_s} - C_w \right) \quad \text{eq1}$$

where V_w (m^3) is the volume of external water in the batch; $k_{s,rev}$ (s^{-1}) is the first-order reversible kinetic sorption rate; $C_{s,rev}$ (moles kg^{-1}) is the reversibly bound pollutant concentration

in soil particles; C_w (moles m^{-3}) is the concentration of pollutant in external water; and K_s (m^3 kg^{-1}) is the partitioning coefficient of the reversibly bound pollutant on soil particles when sorption equilibrium is established.

The irreversible mass transfer rate of the pollutant from external water to soil particles, $r_{s,irrev}$ (moles s^{-1}), is described by

$$r_{s,irrev} = V_w k_{s,irrev} C_w \left(\frac{C_{s,irrev,max} - C_{s,irrev}}{C_{s,irrev,max}}\right) \quad \text{eq2}$$

where $k_{s,irrev}$ (s^{-1}) is the first-order irreversible kinetic sorption rate; $C_{s,irrev}$ (moles kg^{-1}) is the irreversibly bound pollutant concentration in soil particles; $C_{s,irrev,max}$ (moles kg^{-1}) is the maximum irreversibly bound pollutant concentration in the soil particles.

The sorption-retarded intraparticle diffusion mass transfer rate of the pollutant from external water to biochar particles, $r_{ippwd,out}$ (moles s^{-1}), is described by

$$r_{ippwd,out} = N_{p,BC}.4\pi R_{BC}^2.D_{eff,BC}.{}^{\partial}/_{\partial r}\, C_{BC,ippw}\big|_{r=R_{BC}} \quad \text{eq3}$$

where $N_{p,BC}$ (-) is the number of biochar particles; R_{BC} (m) is the biochar particle radius; r (m) is the radial distance from the biochar particle center; and $D_{eff,BC}$ (m^2 s^{-1}) is the effective diffusion coefficient in the biochar pore network defined as:

$$D_{eff,BC} = \frac{\theta_{BC,w}.D_{aq}}{\tau} \quad \text{eq4}$$

where D_{aq} (m^2 s^{-1}) is the molecular diffusion coefficient of the pollutant in water; τ (-) is the biochar pore network tortuosity factor.

The pollutant concentration in biochar intraparticle pore water, $C_{BC,ippw}$ (moles m^{-3}), is governed by the following partial differential equation:

$$\left(\theta_{BC,w} + \left(1 - \theta_{BC,w}\right) d_{BC} K_{BC}\right) \frac{d}{dt} C_{BC,ippw} = \frac{D_{eff,BC}}{r^2} . \frac{\partial}{\partial r}\left(r^2 \frac{\partial}{\partial r} C_{BC,ippw}\right) \qquad \text{eq5}$$

where $\theta_{BC,w}$ (-) is the water-filled intraparticle biochar porosity; d_{BC} (kg m^{-3}) is the skeletal solid density of the biochar; K_{BC} (m^3 kg^{-1}) is the partitioning coefficient of the reversibly pollutant within biochar particles; and t (s) is the time.

For boundary conditions, it is assumed that the pollutant concentration for biochar intraparticle pore water at the external water–biochar interface is equal to the pollutant concentration in the external water phase (no external aqueous film mass transfer resistance).

Based on a mass balance, the pollutant concentration in the external water phase of the batch experiments is governed by the following differential equation:

$$V_w . {}^{d}/_{dt}\, C_w = -r_{ippwd,out} - r_{s,rev} - r_{s,irrev} \qquad \text{eq6}$$

The pollutant distribution between the solids (soil particles and biochar particles) and the external water phase in the batch is described by the apparent sorption coefficient, $K_{d,app}$,:

$$K_{d,app} = \frac{M_{pol} - C_w V_w}{(M_s + M_{BC}) C_w} \qquad \text{eq7}$$

where M_{pol} (moles) is the amount of pollutant added to the batch, M_s (kg) is the total mass of soil particles, and M_{BC} (kg) is the total mass of biochar particles in the batch.

The system of differential equations was solved numerically using the Matlab© differential equation solver ode15 and the method of lines. The input values of the batch kinetic sorption model are presented in Supporting Information in Table S2.

Column leaching numerical model. Figure 2B presents the conceptual column model which simulates the pollutant leaching in the column experiments. This conceptual column is divided into a number of sub-volumes along the one-dimensional vertical downward direction of the flow. Mass transfer processes of the pollutants in every sub-volume are simulated by considering advection and dispersion in addition to the sorption processes discussed in the batch sorption kinetic model (Figure 2A). Based on a mass balance, the following partial differential equation governs the pollutant concentration in the interparticle water phase in between the soil and biochar particles:

$$\theta_w . {}^{d}/_{dt}\, C_w = \theta_w D_{disp}\, {}^{\partial^2}/_{\partial x^2}\, C_w - \theta_w v_x\, {}^{\partial}/_{\partial x}\, C_w - r_{ippwd,out} - r_{s,rev} - r_{s,irrev} \quad \text{eq8}$$

where θ_w (-) is the fraction of the column volume in between the soil and biochar particles, which is assumed to be fully water saturated; D_{disp} ($m^2\ s^{-1}$) is the dispersion coefficient for the pollutant in interparticle water; v_x ($m\ s^{-1}$) is the velocity of this water moving in the x direction.

The interparticle water to biochar particles mass transfer rate, $r_{ippwd,out}$ (moles s^{-1}), is described by

$$r_{ippwd,out} = \frac{\theta_{BC}}{\frac{4}{3}\pi R_{BC}^3} . 4\pi R_{BC}^2 . D_{eff,BC} . {}^{\partial}/_{\partial r}\, C_{BC,ippw}\big|_{r=R_{BC}} \quad \text{eq9}$$

where $C_{BC,ippw}$ is governed by equation eq5 with the same boundary conditions as assumed for the batch model.

The reversible soil pore water to soil particles mass transfer rate, $r_{s,rev}$ (moles s^{-1}), is described by

$$r_{s,rev} = -\theta_w k_{s,rev}\left(\frac{C_{s,rev}}{K_s} - C_w\right) \quad \text{eq10}$$

The irreversible soil pore water to soil particles mass transfer rate, $r_{s,irrev}$ (moles s^{-1}), is described by

$$r_{s,irrev} = \theta_w k_{s,irrev} C_w \left(\frac{C_{s,irrev,max} - C_{s,irrev}}{C_{s,irrev,max}}\right) \quad \text{eq11}$$

As column boundary conditions, it is assumed that (*i*) the pollutant concentration at the column inlet is equal to the concentration of the column influent, and (*ii*) a zero concentration gradient boundary condition is enforced at the column outlet.

The system of differential equations was solved numerically using the Matlab© differential equation solver ode15 and the method of lines. The input values of the column leaching model are presented in the Supporting Information in Table S3.

Model calibration procedures. Input parameters for the batch sorption kinetic model were mostly obtained from the batch experiments and provided in Table S2. For instance, values of K_s (or K_{BC0}) were obtained from the $K_{d,app}$ values after 720 h contact time in BC0 treatments (Table 2). Values of K_{BC} was determined based on the observed $K_{d,app}$ values at 24 h of BC100 treatments and the best-fit with the observed $K_{d,app}$ values of BC1 and BC5 treatments. For the BC100 treatments, only $K_{d,app}$ values at 24 h were measurable, while the values at 168 and 720 h were not measureable because the labeled ^{14}C-concentrations of the pollutants decreased under the detection limit, see Table 3. The $K_{d,app}$ values of BC1 and BC5 treatments were additionally used to determine the

effect of biochar fouling by the soil slurry on the biochar pore network tortuosity (τ_{BC} values in Table 2). Values of $k_{s,rev}$ were determined as the best fit parameters for the soil only (BC0) data by minimizing the sum of squared residuals between the observed and predicted $K_{d,app}$ measured at different contact times.

The first-order irreversible kinetic sorption rates of soil ($k_{s,irrev}$) and the maximum irreversibly sorbed pollutant concentrations on soil particles ($C_{s,irrev,max}$) were derived from the BC0 (soil only) column treatment data by minimizing the sum of squared residuals between the observed and the predicted cumulative pollutant breakthrough data. This irreversible sorption to the soil domain was also considered for the batch experimental data, where it had only minor effects on the predicted $K_{d,app}$ values, and for the other column treatments (BC1, BC5). Other input parameters for the column transport model were obtained from the batch and column experiments, and from the batch numerical model (Table S3).

Results and Discussion

Batch sorption kinetic experiments

Biochar amendment significantly enhanced the apparent partitioning coefficients ($K_{d,app}$) of the three pollutants of SMZ, IPU, and PHE (Figure 3 and Table 3) in the tested soil. In the soil treatments without biochar (BC0), $K_{d,app}$ value of SMZ was smaller than the same values of IPU and PHE after 720 h contact time (Table 2). This is in line with the trends in water solubility (SMZ > IPU > PHE) and the octanol-water partitioning coefficients (SMZ < IPU < PHE) (Table S1). However, in the soil treatments with the highest biochar dose (BC5 with 5% biochar), the $K_{d,app}$ values of IPU and SMZ significantly exceed that value of PHE after 720 h (Table 2). These results suggest that: (*i*) 5% biochar amendment significantly enhance the partitioning coefficients of IPU,

SMZ, and PHE, by factors of 23, 20, and 2, respectively; and (*ii*) the affinity of biochar towards the polar functional groups of IPU and SMZ was higher than the affinity toward the non-functional group compound of PHE. Previous studies in surface chemistry of biochar reported that acidic functional groups e.g. carboxylic and phenolic groups have been found in the structure of biochar.[4, 26, 27] These groups make the surface of biochar highly reactive[28] and enable strong interactions with the polar functional groups of SMZ and IPU. It has been reported that electrostatic interaction is one of the major adsorption mechanisms for SMZ on carbonaceous materials.[29] For less hydrophobic compounds containing certain functional groups, polar and/or H-bonding between biochar and such pollutants may occur, leading to strong sorption of such compounds also to non-activated biochar.[7] Additionally, Graber and Kookana[11] presented that affinity and capacity of most biochars for pesticides generally greatly exceeds those of soil sorbents. The observations are for example consistent with the low sorption capacity of soil[21] and high sorption capacity of biochar amended soil[6] toward IPU. An important study finding is therefore, that biochar amendment not only augments the organic pollutant binding characteristics, but also diversifies the pollutant-soil interaction mechanisms, thus facilitating the retention and reducing the leaching risks for compounds with a range of molecular properties.

On the other hand, the sorption rates of the hydrophobic compound (PHE) were faster than the rates of the hydrophilic compounds (SMZ and IPU). The $K_{d,app}$ values of PHE in BC5 appeared to stabilize during 168 – 720 h contact time, but continued to increase over the duration of the experiments for SMZ and IPU. This is in line with intraparticle diffusion theory which implies that greater sorption (higher K_{BC}) results in slower sorption kinetics. The intraparticle diffusion process of a solute into the microporous structure of pyrogenic carbonaceous materials, e.g. biochar, is retarded by the solute sorption to the pore walls and known to be a long-term process which may

take months or even years to complete.[17, 30] This may explain the continuously increasing trends of $K_{d,app}$ of SMZ, IPU in biochar amended soil treatments (1 – 5% biochar), while the soil only treatments (BC0) equilibrated more quickly in the case of IPU and PHE, although not for SMZ.

Batch sorption kinetic modelling

The temporal changes of $K_{d,app}$ values of SMZ, IPU, and PHE were generally well fitted by the batch sorption kinetic model (Figure 3, solid lines), although there are deviations for the earlier data in some cases. Such deviations, which have also been observed in previous studies [16, 30], could be due to simplifying model assumptions, such as all biochar particles having identical size, or no external aqueous film mass transfer resistance. In intraparticle diffusion theory, the tortuosity factor accounts for the interconnectivity of the pores within biochar particles and provides a fitting parameter for the interpretation of kinetic experiments. It is interesting to observe that the fitted biochar pore network tortuosity factors were: (*i*) generally very high for the hydrophilic compound SMZ (14000 in BC1) and the moderately hydrophobic compound IPU (9000 in BC1) as compared to the strongly hydrophobic PHE (1600 in BC1) and (*ii*) strongly affected by the mixing ratios of biochar in soil since the fitted tortuosity values decreased in the order BC1 > BC5 > BC100 (Table 2). The tortuosity values fitted for the pure biochar (BC100) are in the range of those reported by Ulrich and co-workers [8] for another wood-derived biochar (BN-biochar), but are much higher than those predicted by empirical predictions based on Archie's law for a highly porous particle.[24] Although wood-derived biochars have a highly developed macroporosity (SEM image presented in Figure 1), the diffusion of pollutants into the macropore walls of biochar, which are also visible in the SEM image, and where most of the microporous sorption capacity should be located, appears to be strongly hindered. Mixing of biochar with soil may result in surface coverage and pore blockage by fouling with natural organic matter or the precipitation of solids like carbonates. Pore

blockage by soil constituents may explain the greater fitted tortuosity factors for biochar mixed with soil (BC1, BC5) as compared to the pure biochar (BC100). Pore blockage by carbonates in biochar was previously reported.[3, 10] Furthermore, it was suggested that higher molecular weight organic compounds are more affected by char pore blockages which are caused by condensed deposits of humic substances as compared to lower molecular weight organic substances.[31] This could explain why the magnitude of the apparent fouling effect observed in this study decreased in the order of SMZ > IPU > PHE.

Column leaching experiments

Biochar amendment also significantly reduced the porewater flow rate in the column leaching experiments. Table 2 presented that with 1% and 5% biochar additions (BC1 and BC5 columns), the flow rates were reduced by 57% and 82%, respectively. This is in line with the fine particle size of biochar (Table 1). Previous studies also reported that the saturated conductivity of sandy soil were significantly decreased with the increase of biochar/activated carbon doses.[32-35]

Leaching of the pollutants observed in the column experiments was strongly affected by these kinetic processes. The fraction of the accumulative pollutant mass transported out of the column in relation to the total pollutant mass initially added on the top of the column (M_{out}/M_{in}) was used to examine the transport process of the pollutants (Figure 4). As already observed by Ulrich and co-workers,[8] the qualitative shape of the measured pollutant elution curves is different from those anticipated by a model which assumes local, instantaneous sorption equilibrium between the entire column matrix and the mobile porewater. In reality, the observed pollutant breakthrough is bimodal, with a significant portion of the added pollutant mass breaking through within 0.06 to 0.36 h retention time (or the initial 100-200 ml flush), and most of the remaining

pollutant mass then being very strongly retained by the column matrix. Pollutant retention was verified by showing that the total amount of PHE retained in the column matrix (Figure S2) is significant in comparison to the amount of the PHE flushed out of the columns (Figure 4C) and consistent with the PHE mass originally applied to the system. The bimodal distribution was affected by the biochar amendment, i.e., columns with the highest biochar dose (BC5) retained the greatest portion of the added pollutant mass. This is consistent with the biochar effects on porewater flow rates, showing that the slowest flow rate (BC5, Table 2) gave the longest contact time for adsorption of the pollutants by the solid sorbents.

For SMZ (Figure 4A), 86, 80, and 55 % of the applied mass were transported out of the BC0, BC1, and BC5 columns, respectively, within 0.06 – 0.36 h (100 ml flush). This result indicates that while SMZ was a high mobile contaminant in saturated soil, it was retained significantly better in biochar amended soil (BC5) as compared to soil without biochar (BC0). The high mobility of SMZ in natural soils and the efficiency of biochar amendment to retain this pollutant is consistent with previous studies.[7, 36]

For IPU (Figure 4B), within 0.12 – 0.72 h (200 ml flush) 81, 77, and 44 % of the applied mass were transported out of the BC0, BC1, and BC5 columns, respectively. This indicates also that, although IPU's mobility was rather high in saturated soil, IPU was significantly better retained in the biochar amended soil. Respectively, these observations are consistent with Trinh and co-workers [21] and Reid and co-workers.[6]

For PHE (Figure 4C), within 0.06 – 0.36 h (100 ml flush) only 30, 26, and 16 % of PHE were flushed out of BC0, BC1, and BC5 columns, respectively. This indicated that PHE was already well retained in the soil even in the absence of biochar, but biochar further improved

retention (Figure S2). This is consistent with the high K_s value of PHE ($20.55.10^{-3}$ m^3 kg^{-1}) observed from the BC0 batch experiment (Table 2).

Of the three compounds, PHE was thus retained much more strongly than SMZ and IPU without and with biochar amendment. For instance, in the original soil (BC0) columns, 70 % of PHE was retained in the column versus 14 % and 19 % of SMZ and IPU, respectively; and up-to 84 % of PHE was retained in the BC5 columns versus 45 % and 54 % of SMZ and IPU, respectively. This suggests that, in the context of low biochar amendment doses (up-to 5 %), the extent of retention for different compounds during high flow events is more in line with the trends in their K_s rather than K_{BC} values. Biochar addition nonetheless significantly enhanced the pollutant retention capacity of the columns when comparing the different columns (BC0, BC1, BC5) for a specific compound (Figure 4). This indicates that biochar strongly influenced the transport of the tested compounds, but apparently not solely via its pollutant binding capacity. A numerical mass transfer model was developed to further interpret these intricate experimental observations.

Column transport modelling

Effect of biochar on leaching of the pollutants in biochar-soil system was first simulated by the column transport model which only considered the reversible sorption processes (Figure 4, dashed lines). The simulated outcomes were, however, not consistent with the experimental observation (Figure 4, symbols). Remarkably, the simulations would predict the greatest cumulative breakthrough for PHE after 1000 ml of water passing through the columns (Figure 4C, dashed lines), whereas in fact PHE was observed to be retained the most. In order to better reproduce the bimodal transport behavior and compound-specific trends of the organic pollutants

in these column studies, the numerical model needs to include an irreversible sorption process, with a maximum adsorbed pollutant concentration which can be irreversibly bound. Because the trend in long-term retention was more consistent with K_s rather than K_{BC} values, as mentioned above, irreversible sorption was considered for the original soil matrix. The irreversible sorption rates and the maximum irreversibly adsorbed pollutant concentrations were fitted from the BC0 column studying data. This irreversible sorption to the soil was then re-considered for the modelling of both, the batch and column experiments with the same parameter values, but only had a significant impact on the model predictions for the column study (Figure 4, dashed *vs* solid lines), and not for the batch study (Figure 3, dashed *vs* solid lines). In the column studies, irreversible sorption largely explained the portion of the added pollutant mass retained in the column for the duration of the experiment, although the amount retained is still slightly underestimated. According to the model, the main reason for the greater pollutant mass retained in BC5 column as compared to BC0 column results not so much from the high sorption capacity of biochar, but instead the significant reduction of the infiltration flow rates (from $0.4401.10^{-6}$ m^3 s^{-1} in BC0 column to $0.0773.10^{-6}$ m^3 s^{-1} in BC5 column, Table 2), which is due to the biochar addition. Slower flow provides more retention time for the irreversible sorption process to occur. Irreversible sorption, i.e. irreversible as a minimum over the duration of the experiment, is a necessary component for explaining the qualitative shape of the breakthrough curves in the column study. The phenomenon could be due to very strong adsorption-desorption hysteresis.[37]

Conclusions

Soil amendment with biochar produced from a full-scale wood gasifier enhanced retention in laboratory leaching tests, not only for hydrophobic pollutants (here, PHE), but also for hydrophilic pollutants (here, IPU and SMZ). The column leaching tests suggested that 5% biochar

amendment dose significantly enhanced the pollutant binding and also reduced water infiltration rates in sandy loam soil and thereby reduced pollutant leaching risks during heavy rainfall events. Numerical modelling indicates that pore blockage by soil constituents may reduce biochar sorption capacity, and during high flow events, soil irreversible sorption plays an essential role in the pollutant retention. Overall, these results support the application of the solid biochar co-product of full-scale renewable energy generation as a low-cost sorbent material, but field verification of the laboratory results is required as the next step towards real world applications. This material could be usefully purposed in stormwater filters, buffer strips for agricultural land or in contaminated soils to reduce pollutant leaching.

Acknowledgements. Experimental work was conducted at the University of East Anglia and modelling work was mostly conducted at Newcastle University. Trinh acknowledges the support from the University of East Anglia and Newcastle University.

Supporting Information. Further details of soil, biochar, chemicals, column experimental set-up, and input parameters of the batch and column models are presented in the Supporting Information. This material is available online only.

Corresponding Author

Bao-Son Trinh is a current lecturer at the Institute for Environment and Resources, Vietnam National University of Hochiminh city. He was a research associate at the University of East Anglia and Newcastle University. Email address: son.trinh@newcastle.ac.uk or trinhbao_son@yahoo.com.

Table 1. Physico-chemical properties of the soil and biochar samples

	Soil	Biochar
Particle size distribution (%, by weight)		
- Clay (< 2 µm)	0	0
- Silt (2 – 50 µm)	21	23
- Sand (50 – 2000 µm)	79	77
Geometric mean radius (µm)	165	107
Particle density, (g cm^{-3})	2.49 ± 0.05	1.52 ± 0.04
Bulk density, ρ_b (g cm^{-3})	1.26 ± 0.00	
Bulk porosity, n (%, by volume)	0.49 ± 0.02	
Intraparticle porosity (%, by volume)		0.65 [38]
pH (in distilled water)	7.3	8.9
pH (in $CaCl_2$ 0.01M)	7.0	8.2
Soil water content (%,by weight)	8.2 ± 0.1	
Organic matter content (%,by weight)	3.5 ± 0.2	

Table 2. Kinetic sorption and transport parameters of the organic pollutants in biochar-soil systems obtained from the experimental observations [(o)] and modelling predictions [(p)]; BC0, BC1, BC5, and BC100 denotes 0, 1, 5, and 100% (w/w) of biochar, respectively, in the mixtures with soil.

Pollutants	Partitioning coefficient $.10^{-3}$ (m^3/kg) [(o)] (720 h contact time)				Biochar tortuosity factor [(p)]			Infiltration flow rate $.10^{-6}$ (m^3/s) [(o)]		
	K_{BC0} (or K_s)	K_{BC1}	K_{BC5}	K_{BC100} (or K_{BC})[(p)]	τ_{BC1}	τ_{BC5}	τ_{BC100}	Q_{BC0}	Q_{BC1}	Q_{BC5}
SMZ	3.46	7.35	67.56	1500	14000	1200	300	0.4401	0.1895	0.0773
IPU	6.41	16.81	148.90	4000	9000	1000	400	ab	ab	ab
PHE	20.55	25.56	48.38	600	1600	1500	1000	ab	ab	ab

ab – as above

Table 3. Apparent partitioning coefficient, K_{d_app} of SMZ, IPU, and PHE in soils amended 0, 1, 5 and 100 % (w/w) of biochar (denoted as BC0, BC1, BC5 and BC100, respectively). Error is calculated from the fraction error propagation based on the standard error of the initial concentration ($C_{w,0}$) and the observed concentration (C_w) of the solutes in the aqueous phase (triplicated).[2]

$K_{d\_app}.10^{-3}$ (m^3/kg)	SMZ				IPU				PHE			
Time, h	BC0	BC1	BC5	BC100	BC0	BC1	BC5	BC100	BC0	BC1	BC5	BC100
0.5	0.29±0.64	0.01±0.38	0.54±0.37		1.81±0.45	2.40±0.84	3.84±0.73		9.52±0.50	9.31±0.62	12.60±0.54	
1	0.31±0.54	0.05±0.35	0.69±0.39		2.13±0.32	2.62±0.57	5.00±0.73		9.85±0.73	9.399±0.84	13.35±0.72	
12	0.52±0.33	0.83±0.33	3.13±0.75		2.86±0.39	4.25±0.41	11.21±1.54		13.54±0.86	11.69±0.71	19.23±1.21	
24	0.64±0.25	1.43±0.29	6.79±0.70	785.5±20.9	4.29±0.43	6.99±0.87	59.15±4.94	1047±55	18.29±1.85	18.01±0.25	27.87±1.31	285.6±12.8
168	2.52±0.61	4.58±0.58	40.13±5.17	-	6.43±0.98	10.85±0.61	78.23±2.64	-	19.28±0.54	23.15±0.50	46.49±0.35	-
720	3.46±0.42	7.35±0.39	67.56±7.55	1500 (.)	6.41±0.17	16.81±1.29	148.9±20.17	4000 (*)	20.55±0.29	25.56±0.36	48.38±2.06	600 (*)

(*) Predicted by the batch and column mass transfer numerical models

[2] While errors for $K_{d,app}$ were substantial during the early phase of the equilibration, they significantly reduced to less than 13.5 % after equilibration (720 h).

Figure 1. Scanning electron micrograph images (SEM Jeol JSM-5900LV) at x500 magnification of a soil (A) and biochar (B) particle

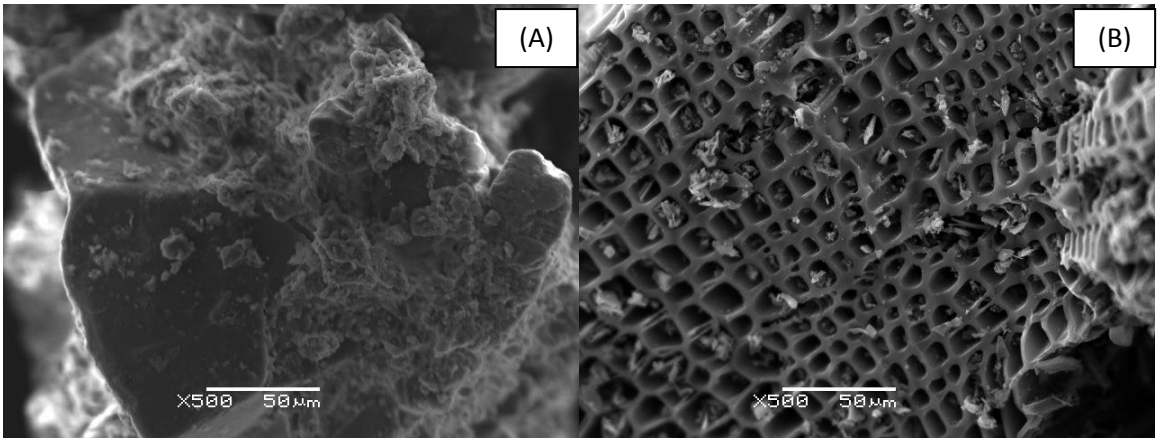

Figure 2. Three-domain, namely biochar, soil, and external water, conceptual models for simulating mass transfer processes of organic pollutants in: **(A)** the batch sorption experiments by assuming (1) reversibly and (2) irreversibly first-order rate kinetic sorption in soil and external water domains; and (3) sorption-retarded intraparticle diffusion in biochar and external water domains; and **(B)** the column leaching experiments by including the mass transfer processes described in Figure (A) in addition to (4) advection and (5) dispersion processes.

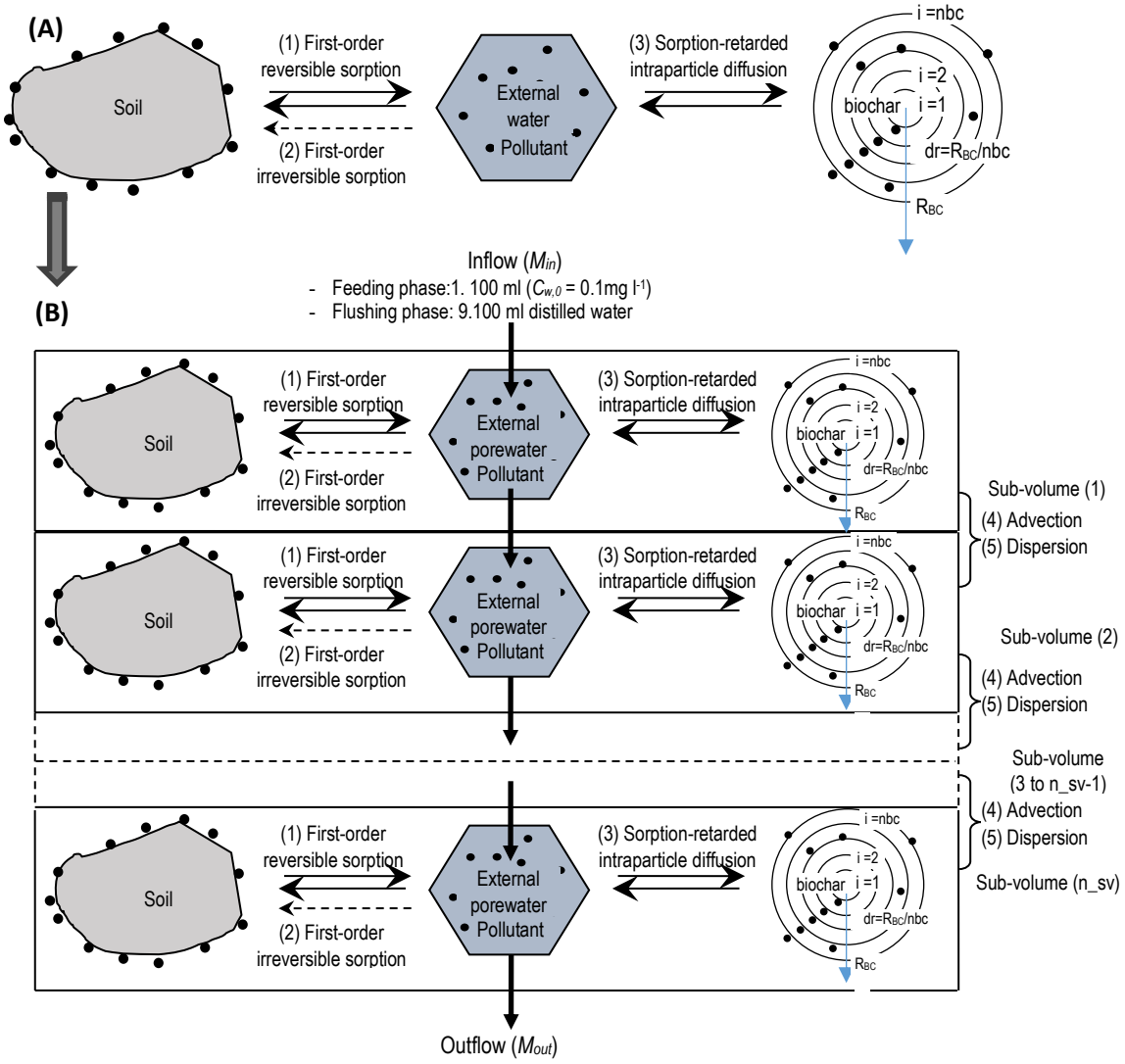

Figure 3. Batch sorption kinetic experiments: observed (symbols) and predicted (solid and dash lines) apparent partitioning coefficient ($K_{d,app}$) with increasing retention time for SMZ (A), IPU (B), and PHE (C). The symbols '○', '◊', 'Δ', and '∗' denote for treatments with 0, 1, 5, and 100% (w/w) of biochar amended soil, respectively. Errors were calculated from the fraction error propagation with standard errors of the initial concentration ($C_{w,0}$) and observed concentration (C_w) of the solutes in the aqueous phase (triplicates). For values of the errors please see Table 3.

1

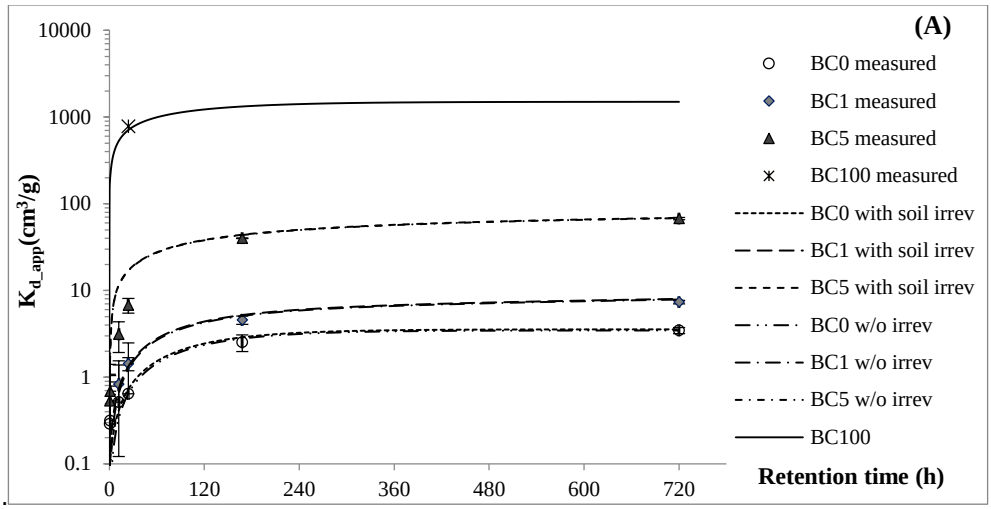
(A)
K_{d_app}(cm³/g)
10000
1000
100
10
1
0.1
0
120
240
360
480
600
720
Retention time (h)
BC0 measured
BC1 measured
BC5 measured
BC100 measured
BC0 with soil irrev
BC1 with soil irrev
BC5 with soil irrev
BC0 w/o irrev
BC1 w/o irrev
BC5 w/o irrev
BC100

2

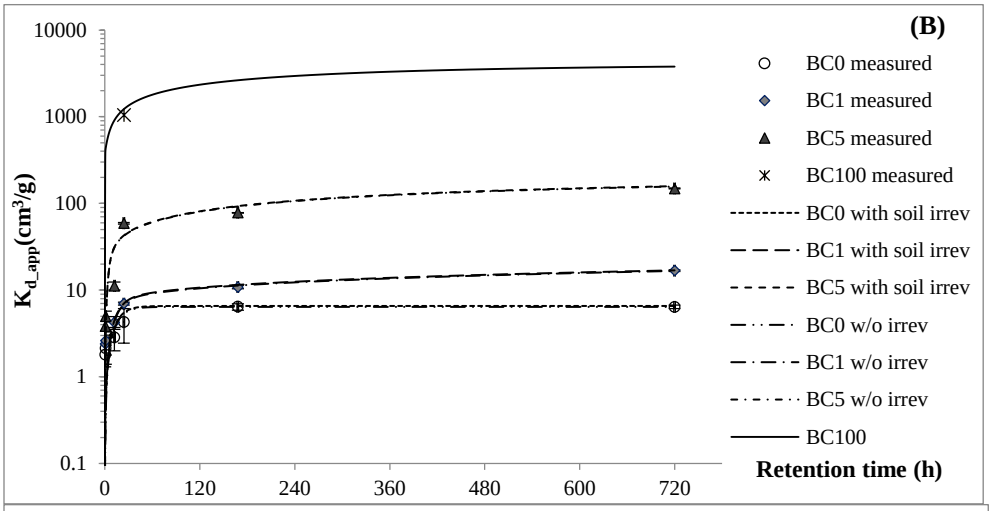
(B)
K_{d_app}(cm³/g)
10000
1000
100
10
1
0.1
0
120
240
360
480
600
720
Retention time (h)
BC0 measured
BC1 measured
BC5 measured
BC100 measured
BC0 with soil irrev
BC1 with soil irrev
BC5 with soil irrev
BC0 w/o irrev
BC1 w/o irrev
BC5 w/o irrev
BC100

3

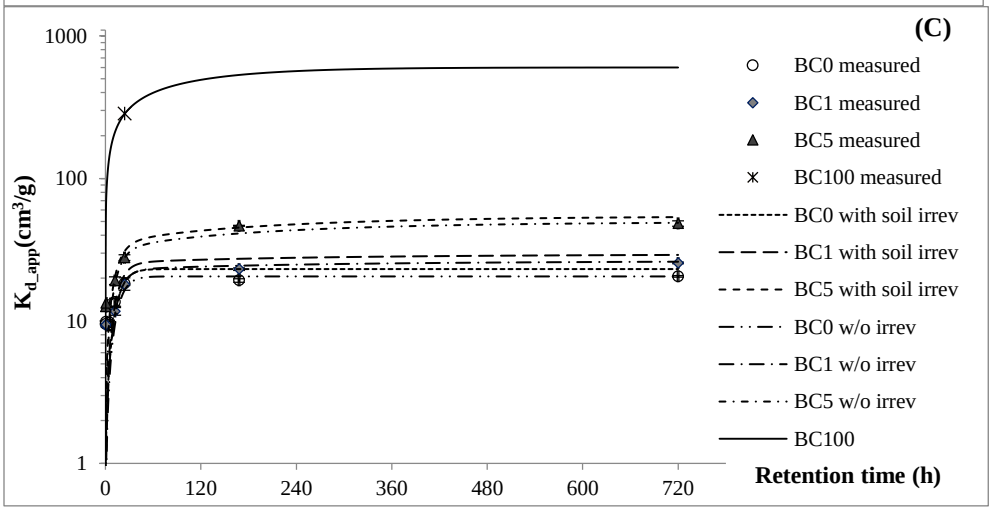
(C)
K_{d_app}(cm³/g)
1000
100
10
1
0
120
240
360
480
600
720
Retention time (h)
BC0 measured
BC1 measured
BC5 measured
BC100 measured
BC0 with soil irrev
BC1 with soil irrev
BC5 with soil irrev
BC0 w/o irrev
BC1 w/o irrev
BC5 w/o irrev
BC100

Figure 4. Column leaching experiments: observed (symbols) and predicted (solid and dash lines) accumulative mass transported-out and -in fractions (M_{out}/M_{in}) of the column with increasing retention time for SMZ (A), IPU (B), and PHE (C). The symbols '○', '◊', and 'Δ' denote for 0, 1 and 5% (w/w) of biochar amended in soil, respectively. Error bars are the standard errors of three replicates (triplicated).

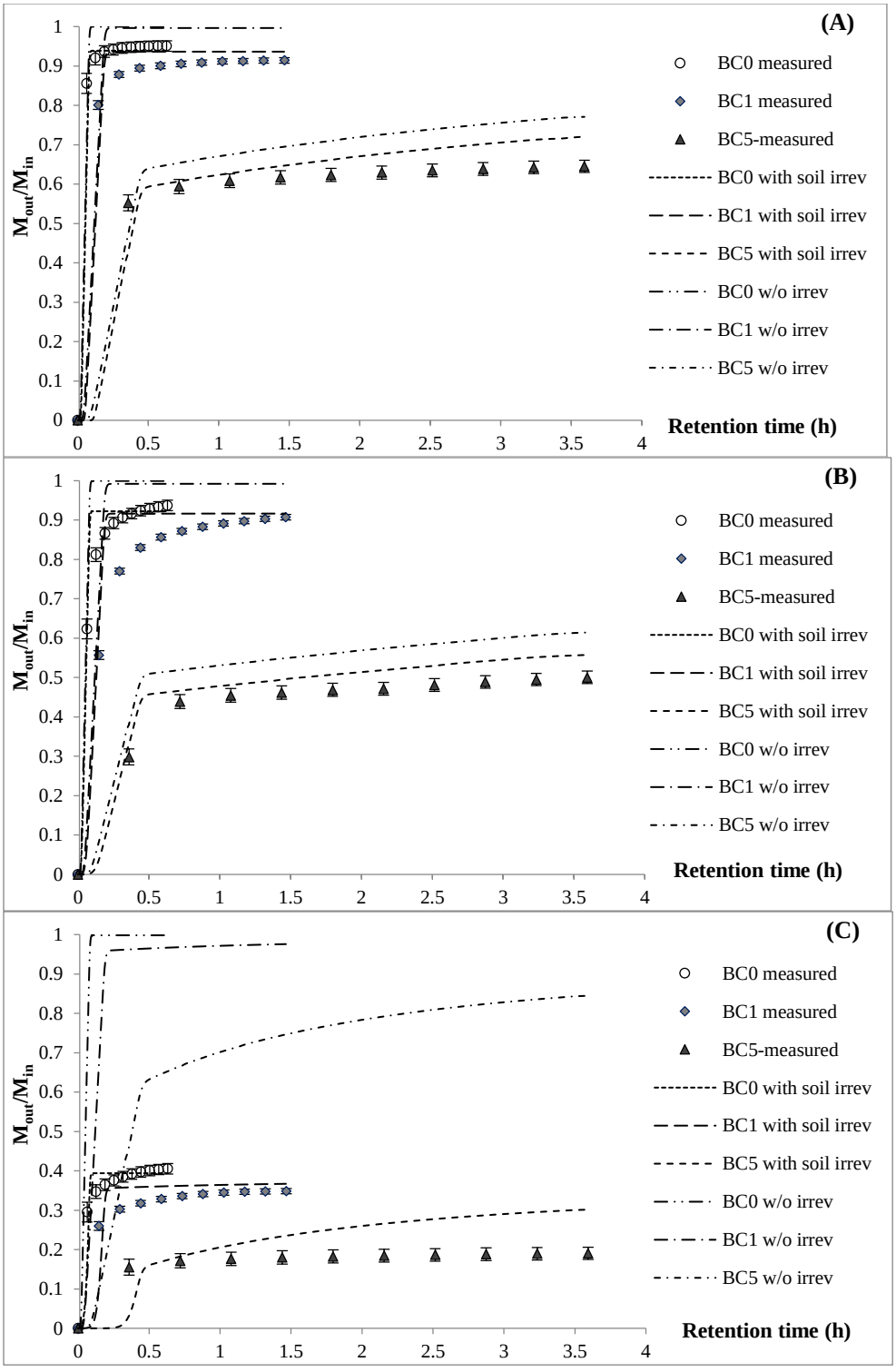

References

1. J Lehmann and aS Joseph, Biochar for Environmental Management: Science, Technology and Implementation. Earthscan, London and New York (2015).
2. HC Chia, A Downie and P Munroe, Characteristics of biochar: physical and structural properties, in Biochar for Environmental Management: Science, Technology and Implementation, ed by J Lehmann and S Joseph. Earthscan from Routledge, London and New York, pp. 89-109 (2015).
3. SE Hale, G Cornelissen and D Werner, Sorption and Remediation of Organic Compounds in Soils and Sediments by (Activated) Biochar, in Biochar for Environmental Management: Science, Technology and Implementation, ed by J Lehmann and S Joseph. Earthscan from Routledge, London and New York, pp. 625-654 (2015).
4. A Mukherjee, AR Zimmerman and W Harris, Surface chemistry variations among a series of laboratory-produced biochars. *Geoderma* **163**: 247-255 (2011).
5. SE Hale, M Elmquist, R Brändli, T Hartnik, L Jakob, T Henriksen, D Werner and G Cornelissen, Activated carbon amendment to sequester PAHs in contaminated soil: A lysimeter field trial. *Chemosphere* **87**: 177-184 (2012).
6. BJ Reid, FL Pickering, A Freddo, MJ Whelan and F Coulon, Influence of biochar on isoproturon partitioning and bioaccessibility in soil. *Environmental Pollution* **181**: 44-50 (2013).
7. M Teixidó, C Hurtado, JJ Pignatello, JL Beltrán, M Granados and J Peccia, Predicting Contaminant Adsorption in Black Carbon (Biochar)-Amended Soil for the Veterinary Antimicrobial Sulfamethazine. *Environmental Science & Technology* **47**: 6197-6205 (2013).
8. BA Ulrich, EA Im, D Werner and CP Higgins, Biochar and Activated Carbon for Enhanced Trace Organic Contaminant Retention in Stormwater Infiltration Systems. *Environmental Science & Technology* **49**: 6222-6230 (2015).
9. Y Chai, RJ Currie, JW Davis, M Wilken, GD Martin, VN Fishman and U Ghosh, Effectiveness of Activated Carbon and Biochar in Reducing the Availability of Polychlorinated Dibenzo-p-dioxins/Dibenzofurans in Soils. *Environmental Science & Technology* **46**: 1035-1043 (2012).
10. Z Han, B Sani, W Mrozik, M Obst, B Beckingham, HK Karapanagioti and D Werner, Magnetite impregnation effects on the sorbent properties of activated carbons and biochars. *Water Research* **70**: 394-403 (2015).
11. RE Graber and SR Kookana, Biochar and Retention/Efficacy of Pesticides, in Biochar for Environmental Management: Science, Technology and Implementation, ed by J Lehmann and S Joseph. Earthscan from Routledge, London and New York (2015).
12. A Fichthorn, B Rehe and D Myers, An innivative solution to a difficult stormwater problem (2014).
13. U Ghosh, RG Luthy, G Cornelissen, D Werner and CA Menzie, In-situ Sorbent Amendments: A New Direction in Contaminated Sediment Management. *Environmental Science & Technology* **45**: 1163-1168 (2011).
14. G Cornelissen, K Amstaetter, A Hauge, M Schaanning, B Beylich, JS Gunnarsson, GD Breedveld, AMP Oen and E Eek, Large-Scale Field Study on Thin-Layer Capping of Marine PCDD/F-Contaminated Sediments in Grenlandfjords, Norway: Physicochemical Effects. *Environmental Science & Technology* **46**: 12030-12037 (2012).
15. KM Bushnaf, S Puricelli, S Saponaro and D Werner, Effect of biochar on the fate of volatile petroleum hydrocarbons in an aerobic sandy soil. *Journal of Contaminant Hydrology* **126**: 208-215 (2011).

16. SE Hale and D Werner, Modeling the Mass Transfer of Hydrophobic Organic Pollutants in Briefly and Continuously Mixed Sediment after Amendment with Activated Carbon. *Environmental Science & Technology* **44**: 3381-3387 (2010).
17. D Werner, U Ghosh and RG Luthy, Modeling Polychlorinated Biphenyl Mass Transfer after Amendment of Contaminated Sediment with Activated Carbon. *Environmental Science & Technology* **40**: 4211-4218 (2006).
18. Y-M Cho, D Werner, Y Choi and RG Luthy, Long-term monitoring and modeling of the mass transfer of polychlorinated biphenyls in sediment following pilot-scale in-situ amendment with activated carbon. *Journal of Contaminant Hydrology* **129–130**: 25-37 (2012).
19. P Meynet, E Moliterni, RJ Davenport, WT Sloan, JV Camacho and D Werner, Predicting the effects of biochar on volatile petroleum hydrocarbon biodegradation and emanation from soil: A bacterial community finger-print analysis inferred modelling approach. *Soil Biology and Biochemistry* **68**: 20-30 (2014).
20. K-R Kim, G Owens, S-I Kwon, K-H So, D-B Lee and Y Ok, Occurrence and Environmental Fate of Veterinary Antibiotics in the Terrestrial Environment. *Water, Air, & Soil Pollution* **214**: 163-174 (2011).
21. SB Trinh, KM Hiscock and BJ Reid, Mechanistic insights into the role of river sediment in the attenuation of the herbicide isoproturon. *Environmental Pollution* **170**: 95-101 (2012).
22. U.S. EPA, Available:http://www.epa.gov/epawaste/hazard/wastemin/priority.htm (accessed 18.01.15.). (2015).
23. U.S. EPA, Methods, Issues, and Criteria for Measuring K_d Values. In: Wilhelm G. R. and Beam P. (Eds) Understanding Variation in Partition Coefficient, K_d, Values, Vol I: The K_d Model, Methods of Measurement, and Application of Chemical Reaction Codes, in EPA 402-R-99-004A US Environmental Protection Agency, Washington, DC (1999).
24. P Grathwohl, Diffusion in natural porous media: contaminant transport, sorption/desorption and dissolution kinetics. Kluwer Academic, Massachusetts, MA (1998).
25. D Werner, HK Karapanagioti and DA Sabatini, Assessing the effect of grain-scale sorption rate limitations on the fate of hydrophobic organic groundwater pollutants. *Journal of Contaminant Hydrology* **129–130**: 70-79 (2012).
26. S Hale, K Hanley, J Lehmann, A Zimmerman and G Cornelissen, Effects of Chemical, Biological, and Physical Aging As Well As Soil Addition on the Sorption of Pyrene to Activated Carbon and Biochar. *Environmental Science & Technology* **45**: 10445-10453 (2011).
27. M Teixidó, JJ Pignatello, JL Beltrán, M Granados and J Peccia, Speciation of the Ionizable Antibiotic Sulfamethazine on Black Carbon (Biochar). *Environmental Science & Technology* **45**: 10020-10027 (2011).
28. EJ Amonette and S Joseph, Characteristics of Biochar: Microchemical Properties, in Biochar Environmental Management: Science and Technology, ed by J Lehmann and S Joseph. Earthscan, London-Sterling, VA, pp. 33-52 (2009).
29. Q Yang, G Chen, J Zhang and H Li, Adsorption of sulfamethazine by multi-walled carbon nanotubes: effects of aqueous solution chemistry. *RSC Advances* **5**: 25541-25549 (2015).
30. S Ahn, D Werner, HK Karapanagioti, DR McGlothlin, RN Zare and RG Luthy, Phenanthrene and Pyrene Sorption and Intraparticle Diffusion in Polyoxymethylene, Coke, and Activated Carbon†. *Environmental Science & Technology* **39**: 6516-6526 (2005).
31. JJ Pignatello, S Kwon and Y Lu, Effect of Natural Organic Substances on the Surface and Adsorptive Properties of Environmental Black Carbon (Char): Attenuation of Surface Activity by Humic and Fulvic Acids. *Environmental Science & Technology* **40**: 7757-7763 (2006).
32. AE Ajayi, D Holthusen and R Horn, Changes in microstructural behaviour and hydraulic functions of biochar amended soils. *Soil and Tillage Research* **155**: 166-175 (2016).

33. RT Barnes, ME Gallagher, CA Masiello, Z Liu and B Dugan, Biochar-Induced Changes in Soil Hydraulic Conductivity and Dissolved Nutrient Fluxes Constrained by Laboratory Experiments. *PLoS ONE* **9**: e108340 (2014).
34. SR Brockhoff, NE Christians, RJ Killorn, R Horton and DD Davis, Physical and Mineral-Nutrition Properties of Sand-Based Turfgrass Root Zones Amended with Biochar. *Agronomy Journal* **102** (2010).
35. KC Uzoma, M Inoue, H Andry, A Zahoor and E Nishihara, Influence of biochar application on sandy soil hydraulic properties and nutrient retention. *J Food Agric Environ* **9**: 1137-1143 (2011).
36. M Vithanage, AU Rajapaksha, X Tang, S Thiele-Bruhn, KH Kim, S-E Lee and YS Ok, Sorption and transport of sulfamethazine in agricultural soils amended with invasive-plant-derived biochar. *Journal of Environmental Management* **141**: 95-103 (2014).
37. Y Lu and JJ Pignatello, Demonstration of the "Conditioning Effect" in Soil Organic Matter in Support of a Pore Deformation Mechanism for Sorption Hysteresis. *Environmental Science & Technology* **36**: 4553-4561 (2002).
38. CE Brewer, VJ Chuang, CA Masiello, H Gonnermann, X Gao, B Dugan, LE Driver, P Panzacchi, K Zygourakis and CA Davies, New approaches to measuring biochar density and porosity. *Biomass and Bioenergy* **66**: 176-185 (2014).